

Separation and Structural Characteristics of Lignin in the Prehydrolysis Liquor of *Whangee* Dissolving Pulp

Ruiping Tong, Chaojun Wu,* Chuanshan Zhao, and Dongmei Yu

Separation and structural characterization of lignin are essential for value-added utilization of hemicelluloses and lignin in the prehydrolysis liquor (PHL) of a kraft-based *Whangee* (a genus of bamboo) dissolving pulp production. In this work, lignin in the PHL was separated by acidification treatment (AT) and rotary vacuum evaporation treatment (RVET), and the separated crude lignin was then compared and characterized. The crude lignin separated by RVET could be justified as p-hydroxyphenyl (H) -syringyl (S) -guaiacyl (G) lignin, and a conjugated carbonyl was also found in it. The crude lignin separated by AT was mainly composed of S lignin that had β -1, β -5, β -O-4, and β - β bonds. Thermogravimetric analysis (TGA) showed that the maximum thermal decomposition temperatures and the final carbon residues of crude lignin separated by RVET and AT were 520 °C, 5.26%, and 470 °C, 27.92%, respectively. Moreover, of the five kinds of sugar (arabinose, galactose, glucose, xylose and mannose) in the PHL, only galactose and glucose were decreased after AT, while all five kinds were decreased after RVET.

Keywords: Separation; Structure characteristics; Lignin; Prehydrolysis liquor; *Whangee* dissolving pulp

Contact information: Key Lab of Paper Science and Technology of Ministry of Education, Qilu University of Technology, Ji'nan, China; *Corresponding author: chaojunwu2007@163.com

INTRODUCTION

Prehydrolysis is an important step in the kraft-based dissolving process for dissolving pulp production, as it helps remove as much hemicellulose as possible from cellulose fibers before the material is subjected to the main delignification operation, *i.e.*, pulping (Tong *et al.* 2016). As one of the undesirable components of dissolving pulp, hemicellulose causes several problems in downstream conversion processes and adversely affects the final quality of cellulose derivatives (Zhao *et al.* 2017). Christov and Prior (1993) reported that part of the hemicelluloses (mainly xylan) remains in the pulp after bleaching, thus causing problems at the later alkalization and spinning stages of the viscose process. Significantly, in the prehydrolysis process, a part of lignin is also dissolved in the prehydrolysis liquor (PHL) (Yang and Jahan 2013). The hemicelluloses derived saccharides can be converted into high value-added chemicals such as xylitol and ethanol. However, the presence of lignin inhibits the production of xylitol and ethanol (Wang *et al.* 2014, 2015a). Therefore, it is important to effectively enhance the separation of lignin from the PHL. Once separated from the PHL, lignin itself can be a raw material for many value-added products, *e.g.*, phenols, biofuel, and plastics (Wang *et al.* 2014). Of the non-woods, bamboo is considered to be one of the most attractive feedstocks due to its rapid growth and similar chemical composition to that of woods (Yuan *et al.* 2016, 2017; Zhao *et al.* 2017). Furthermore, ideal bamboo dissolving pulp with high brightness (92.4% ISO) and α -cellulose content (94.9%) has been obtained (Batalha *et al.* 2011). The objective of this paper was to characterize the lignin in the PHL obtained from *Whangee* (a genus of bamboo)

dissolving pulp, so that its subsequent utilization in the production of value-added products or its efficient separation from PHL will be facilitated.

The characteristics of lignin vary among the type and intensity of the delignification process, lignocellulosic materials, and even within tissues of the same individual plant (Jahan and Mun 2007; Wen *et al.* 2015). Shuai *et al.* (2016) reported that pretreatment processes using high temperatures and/or mineral acids lead to lignin condensation, lignin ether bond cleavage, and stable carbon-carbon bond formation. Presently, various lignin, such as milled wood lignin and acetic acid lignin, separated from raw materials or solid residues have been prepared and studied, while the lignin samples in liquor have been prepared mainly by H₂SO₄ precipitation (Hu *et al.* 2013; Shi *et al.* 2013; Yang and Jahan 2013). Shi *et al.* (2013) indicated that the bamboo lignin fractions separated by ethanol had lower weight-average molecular weight compared with aqueous alkaline solutions. Lignin extracted from black liquor shows a different chemical structure than natural lignin due to the unavoidable hydrolysis, condensation, and oxidation reactions during pulping (Hu *et al.* 2013). Yang and Jahan (2013) reported that the lignin of wood separated from PHL by H₂SO₄ precipitation had a significant increase in the phenolic hydroxyl content. From above perspectives, lignin structure and its characterization under various treatments should be studied for lignin chemistry and utilization.

To date, few studies have been carried out on the structural characteristics of lignin in PHL, especially the lignin in the PHL of *Whangee* dissolving pulp. Therefore, structural characteristics of lignin in the PHL obtained from *Whangee* dissolving pulp were investigated in the present study. In this work, lignin in the PHL was simply separated by acidification treatment (AT) and rotary vacuum evaporation treatment (RVET). The separated acid and evaporative precipitate, as crude lignin separated by AT and RVET from PHL, respectively, were compared and characterized by Fourier transform infrared spectroscopy (FTIR), ¹H-NMR spectroscopy, thermogravimetric analysis (TGA), and pyrolysis-gas chromatography/mass spectrometry (Py-GC/MS). Furthermore, the effects of AT and RVET on the chemical compositions in PHL were also determined.

EXPERIMENTAL

Materials and Water Prehydrolysis Process

The raw material of *Whangee*, which included 19.78% pentosan, 73.99% holocellulose, 44.52% α -cellulose, 1.94% acid-soluble lignin, and 20.08% acid-insoluble lignin, was provided by a forestry center in Sichuan province, China (Tong *et al.* 2016). Chipped *Whangee* was screened to obtain chips with a size of 11 mm \times 25 mm \times 6 mm. A portion of *Whangee* chip was taken for moisture determination for subsequent experiments.

Water prehydrolysis was carried out in an electrically heated stainless steel digester (15 L) with 1.2 kg oven dried *Whangee* chips at a constant cooking temperature of 165 °C, and it was heated from room temperature at a heating rate of 8 °C/5 min. The time when cooking temperature was established was 90 min, with a liquor-to-*Whangee* ratio of 8:1. At the end, the digester was cooled and depressurized, and the reaction mixture was withdrawn. The PHL was separated and collected from the water-treated *Whangee* chips. The collected PHL was filtered using one-tier of slowly quantitative filter paper prior to subsequent experiments.

Separation of Crude Lignin by Acidification Treatment

The previous study showed that the formaldehyde could stabilize lignin in an acidic environment (Shuai *et al.* 2016). Therefore, before the PHL acidified, 1 mL of formaldehyde was added in 1 L of PHL. The PHL was acidified to pH 2 using 10% H₂SO₄ solutions, and acid precipitate was separated by centrifugation at 5000 rpm (Yang and Jahan 2013). The acid precipitate as crude lignin was thoroughly washed with distilled water by repeated centrifugation to neutrality and dried in vacuum over P₂O₅. The supernatant was collected from the acidified PHL as PHL1.

Separation of Crude Lignin by Rotary Vacuum Evaporation Treatment

The main mechanism of RVET for evaporative precipitate was concentration. The 200 mL PHL was concentrated to 20 mL in a rotary vacuum evaporator at 50 °C, 0.07 ± 0.01 MPa, and the evaporative precipitate was separated from the concentrated PHL. The evaporative precipitate as crude lignin was dried in vacuum over P₂O₅ and the volume of the concentrated PHL was increased to 200 mL by adding distilled water as PHL2.

Analysis Methods of the Crude Lignin

FTIR spectroscopy

The crude lignin was characterized by Fourier transform infrared spectroscopy (IRPrestige-21, Shimadzu, Kyoto, Japan). The dried samples were embedded in KBr pellets at concentrations of about 1 mg/100 mg KBr. The spectra was recorded in the absorption band mode in the 4000 cm⁻¹ to 400 cm⁻¹ range.

¹H-NMR

The ¹H-NMR spectra were recorded on a 400 MHz Bruker AVANCE III NMR spectrometer (Karlsruhe, Germany). Samples of 20 mg were completely dissolved in 500 μL of dimethyl sulphoxide (DMSO-d₆). The chemical shifts were calibrated relative to the signals of DMSO, which was used as an internal standard at 2.49 ppm for the ¹H-NMR spectra. The acquiring time (AQ) was 3.98 s, and the relaxation time was 1.0 s

Thermogravimetric analysis (TGA)

The crude lignin was characterized by a thermogravimetric analyzer (TGA Q50, TA Instruments, New Castle DE, USA). In the TGA experiment, about 3 mg of samples were pyrolyzed from room temperature to 800 °C at a heating rate of 15 °C/min under N₂ atmosphere.

Pyrolysis-gas chromatography/mass spectrometry (Py-GC/MS)

The Py-GC/MS system included a JHP-3 model Curie-point pyrolyzer (CDS5200, Oxford, PA, USA) and an Agilent 7890B-5977A GC-MS (Santa Clara, CA, USA). Approximately 0.1 mg of samples were pyrolyzed at a certain temperature for 15 s, and the gas products were purged by high purity helium (99.9995%) into the gas chromatograph *via* a transfer line preheated to 270 °C. The flow rate of the carrier gas was 75 mL/min with a split ratio of 50:1. The injection temperature was 270 °C.

The pyrolysis products were separated in a HP-5MS capillary column (30 m × 0.25 mm × 0.25 μm). The GC oven was kept at 50 °C for 2 min and then heated from 50 °C to 270 °C with a heating rate of 10 °C/min. The temperature was then maintained for 3 min. The injector temperature was set at 280 °C in split mode with split ratio of 50:1. The MS detector was operated in electron impact (EI) ionization mode (70 eV) with the ion source

temperature and quadrupole temperature set to 230 °C and 150 °C, respectively. The mass range of 45 m/z to 500 m/z was scanned. The pyrolysis compounds were identified by comparison of their mass fragments with the NIST mass spectral library (NIST 14).

Characteristics Analysis of Original and Treated PHL

Total solid content in PHLs was determined by weighing aliquots of solution before and after oven drying (Chen *et al.* 2014). The sugars were measured using an indirect method based on quantitative acid hydrolysis of the liquid sample. To convert oligomeric sugars to monomeric sugars, the original and treated PHL were hydrolyzed with 4% (wt.) H₂SO₄ at 121 °C for 60 min in an oil bath (Shen *et al.* 2011). The hydrolyzed PHL was filtered (0.22 µm) and the supernatant was used for the determination of monomeric sugars and acid-soluble lignin (Chen *et al.* 2014). The monomeric sugar contents in the post-acid hydrolysate represented the total sugars in both the original and treated PHL. The monomeric sugars were measured using high performance anion exchange chromatography coupled with a pulsed amperometric detector (HPAEC-PAD) and an HPAEC-PAD system (ICS-5000, Thermo Fisher, Sunnyvale, CA) equipped with a CarboPac PA20 analytical column. A guard column was used for MS determination (Wang *et al.* 2015b). The acid-soluble lignin content in the PHL was measured using a UV/Vis spectrometric method at a wavelength of 205 nm according to TAPPI UM 250 (2000) (Shen *et al.* 2011; Shi *et al.* 2011).

Equations

Arabinose was calculated as follows,

$$\frac{\text{Arabinose content in the original PHL} - \text{Arabinose content in the treated PHL}}{\text{Total solid in the original PHL} - \text{Total solid in the treated PHL}} \times 100\% \quad (1)$$

Galactose, glucose, xylose, mannose, total sugars, and acid-soluble lignin contents in the acid and evaporative precipitate were calculated in the same way (Tong *et al.* 2016; Zhou *et al.* 2016).

RESULTS AND DISCUSSION

Calculated Main Composition Content in the Crude Lignin

The acid and evaporative precipitate, which was defined as crude lignin, was separated by AT and RVET from PHL, respectively. To investigate the characteristics of lignin in PHL, the effects of AT and RVET on the chemical composition of PHLs (Table 1) were studied for determining the calculated composition contents in acid and evaporative precipitate (Table 2). A previous study showed that acid-soluble lignin was the major lignin in the PHL; thus only acid-soluble lignin was measured in this work (Tong *et al.* 2016). The pH value of the original PHL was 3.65, whereas PHL2 had a higher pH value of 3.88. Previously, Tong *et al.* (2016) reported that the formic acid, acetic acid and furfural concentrations in PHL obtained from *Whangee* by autohydrolysis were 1.81 g/L, 2.20 g/L, and 0.41 g/L, respectively. Thus, the higher pH value of PHL2 may reflect that furfural and other volatile substances can be removed with heat (Nigam 2001).

The effects of AT and RVET on sugars and acid-soluble lignin concentration in PHLs had taken the volume difference of PHLs into account. As shown in Table 1, sugar, which accounted for over 71% of the total solids, was the main component in PHLs. Xylose and glucose were the predominant sugars in the PHLs. Remarkably, only the galactose and glucose were decreased after AT (Table 1). This may be explained as the arabinose, xylose, and mannose in the PHL were less affected during the AT. However, five kinds of sugar (arabinose, galactose, glucose, xylose and mannose) contents in the PHL were all decreased after RVET (Table 1), which implied that all the components in the PHL were concentrated and partly precipitated out. As shown in Table 2, calculated total sugars and calculated acid-soluble lignin were the predominant components in the acid (85.18%) and evaporative precipitate (85.03%). Notably, acid precipitate had a higher calculated acid-soluble lignin content (37.96%) and a higher ratio (44.56%) of calculated acid-soluble lignin content over the sum of calculated acid-soluble lignin and calculated sugar content to evaporative precipitate. This contributed to the subsequent study of the crude lignin separated by AT. The evaporative precipitate acquired under mild conditions (50 °C, 0.07 ± 0.01 Mpa) may be more representative of lignin in the PHL compared with acid precipitate. And then the treated PHLs can be further treated, such as by adding laccase and polymer (Wang *et al.* 2014), to take full advantage of xylose/xylan fermentation for ethanol or xylitol production.

Table 1. Effect of AT and RVET on Sugars and Acid-soluble Lignin Concentration in PHLs

Sample	Original PHL	PHL1	PHL2
Arabinose (g/L)	0.80	0.80	0.78
Galactose (g/L)	0.79	0.78	0.75
Glucose (g/L)	12.96	12.46	12.29
Xylose (g/L)	10.98	10.98	10.96
Mannose (g/L)	0.38	0.38	0.28
Total sugars (g/L)	25.91	25.40	25.06
Acid-soluble lignin (g/L)	3.12	2.71	2.72
Total solid (g/L)	36.14	35.06	34.67
Total sugars/Total solid (%)	71.69	72.45	72.28
(Glucose+Xylose)/Total sugars (%)	92.40	92.28	92.78

Table 2. Calculated Composition Contents in the Acid and Evaporative Precipitate, as Crude Lignin Separated by AT and RVET from PHL, respectively

	Acid Precipitate	Evaporative Precipitate
Calculated arabinose (%)	0	1.36
Calculated galactose (%)	0.92	2.72
Calculated glucose (%)	46.30	45.58
Calculated xylose (%)	0	1.36
Calculated mannose (%)	0	6.80
Calculated total sugars (T) (%)	47.22	57.82
Calculated acid-soluble lignin (A) (%)	37.96	27.21
A+T (%)	85.18	85.03
A/(A+T) (%)	44.56	32.0

Structural Characteristics Analysis of Crude Lignin

FTIR spectroscopy

The FTIR spectra of acid and evaporative precipitate, as crude lignin separated by AT and RVET from PHL, respectively, are presented in Fig. 1, and the assignments are

listed in Table 3 in accordance with previous papers (Buta *et al.* 1989; Jahan and Mun 2007; Zheng *et al.* 2012; Yang and Jahan 2013; Zhao *et al.* 2014; Constant *et al.* 2015; Li 2016). As shown in Fig 1, all crude lignin had a wide absorption band at 3410 cm^{-1} caused by the O-H stretching vibration of hydroxyl groups, which represented the typical function group of lignin (Huang *et al.* 2012).

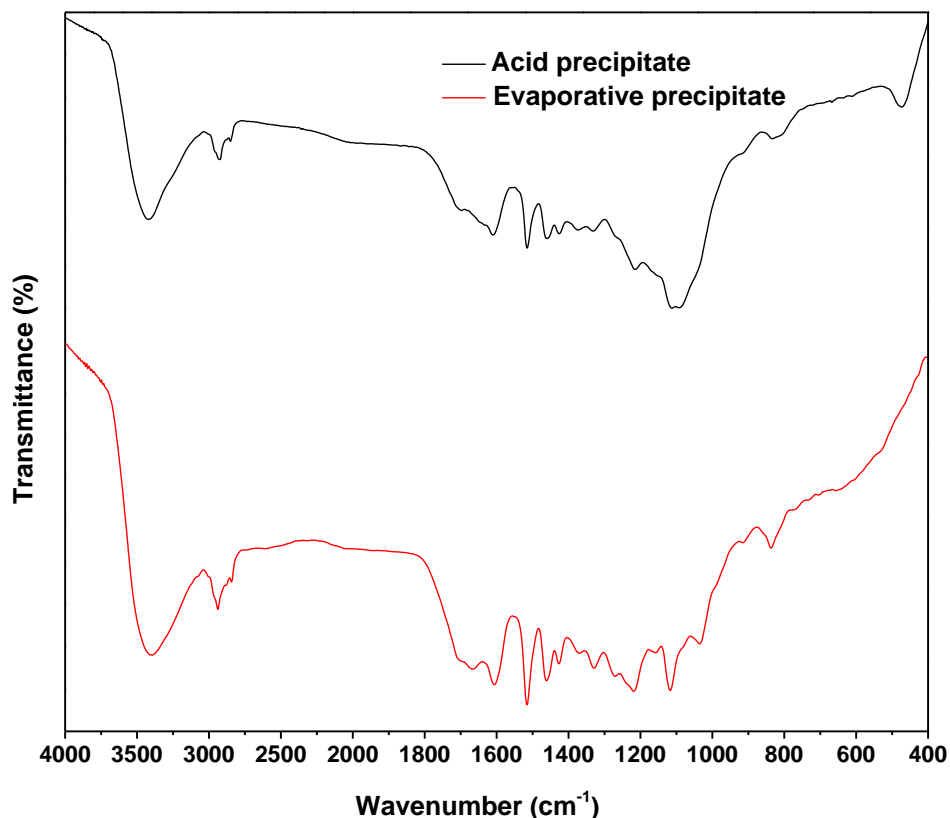


Fig. 1. FTIR spectra of the acid and evaporative precipitate, as crude lignin separated by AT and RVET from PHL, respectively

Table 3. Assignment of FTIR Spectra of Acid and Evaporative Precipitate, as Crude Lignin Separated by AT and RVET from PHL, respectively

Wavenumbers (cm ⁻¹)	Assignment (bond)	Evaporative Precipitate	Acid Precipitate
3410	O-H stretching vibration	3410	3410
2924	C-H stretching vibration in methyl, methylene	2924	2924
1605,1515	Aromatic ring skeleton vibration	1605,1515	1605,1515
1459	C-H deformation vibration in -CH ₂ -	1459	1459
1431	C-H bending vibration in -CH ₂ - of cellulose	1431	1431
1370-1372	O-H deformation vibration of phenol or C-H deformation vibration in CH ₃ -	1372	1372
1330,1220	C-O stretching vibration of syringol units	1330,1220	1330,1220
1269	C-O stretching vibration of guaiacyl units	1269	-
1156	Typical for the coumaric acid ester	1156	-
1107	C-O vibration of carbohydrate	1107	1107
1035	C-H bending vibration of guaiacyl units or C-O bending vibration of primary alcohol	1035	-
835	C-H stretching vibration of syringyl units	835	835

The bands located at 1330 cm^{-1} , 1220 cm^{-1} , 835 cm^{-1} , 1269 cm^{-1} , 1035 cm^{-1} , and 1156 cm^{-1} (Table 3) in evaporative precipitate indicated the existence of syringyl (S), guaiacyl (G), and p-hydroxyphenyl (H) units in crude lignin separated by RVET. In contrast, only the syringyl unit existed in crude lignin separated by AT due to the absence of bands at 1269 cm^{-1} , 1035 cm^{-1} , and 1156 cm^{-1} in acid precipitate. The signals at 1515 cm^{-1} and 1605 cm^{-1} represented the aromatic ring skeleton. Evaporative and acid precipitate spectra showed absorption of the highest intensity at 1515 cm^{-1} and 1107 cm^{-1} , respectively. The lower intensity of the band at 1515 cm^{-1} in acid precipitate, and the higher calculated acid-soluble lignin content (Table 1) than that of evaporative precipitate further indicated that the highest syringyl unit content was in crude lignin separated by AT. As shown in the evaporative precipitate spectra, higher intensity of the bands at 1220 cm^{-1} and 1330 cm^{-1} than 1269 cm^{-1} and 1035 cm^{-1} , respectively, compared with the lowest intensity of the band at 1156 cm^{-1} indicated the highest syringyl unit content and the lowest p-hydroxyphenyl unit content in crude lignin separated by RVET. The highest syringyl unit content in crude lignin separated by AT and RVET indicated quite possibly that the lignin in the PHL was mainly composed of S lignin.

¹H-NMR

The integrated ¹H-NMR spectra obtained for acid and evaporative precipitate is presented in Fig. 2, with Table 4 listing the positions of signals assigned by previous papers (Lundquist *et al.* 1979; Liu and Duan 1996; Jahan and Mun 2007; Yang and Jahan 2013).

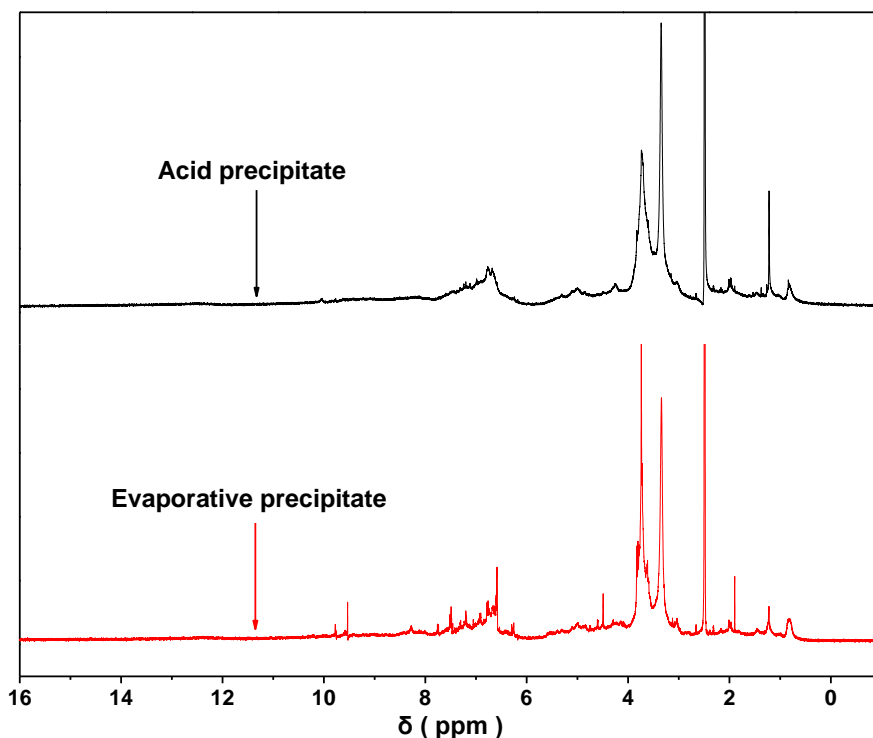


Fig. 2. ¹H-NMR spectra of the acid and evaporative precipitate, as crude lignin separated by AT and RVET from PHL, respectively

Zhang (2016) reported that the signal associated with hemicelluloses was at 3.0 ppm to 5.6 ppm, and that the corresponding signals for the xylose unit were 3.0 ppm to 4.5 ppm. As shown in the evaporative precipitate spectra, the crude lignin separated by RVET

could be justified as HSG lignin, which was indicated by signals at 7.49 ppm to 7.76 ppm, 6.59 ppm to 6.78 ppm, and 7.20 ppm, respectively, and the conjugated carbonyl (9.53 ppm to 9.78 ppm) was also found in it. The presence of conjugated carbonyl could be due to the fact that the quinoids in lignin are destroyed at high temperature and give rise to compounds with carbonyl functional groups during the prehydrolysis process. As shown in the acid precipitate spectra, the crude lignin separated by AT was mainly composed of S lignin, due to the fact that only the syringyl unit (6.77 ppm to 6.79 ppm) was apparent. In addition, calculated galactose and calculated glucose of the calculated total sugars in crude lignin separated by AT (Table 4) and the presence of signal at 4.24 ppm to 4.26 ppm in acid precipitate spectra indicated that the S lignin had β -1, β -5, β -O-4, and β - β bonds. Leschinsky *et al.* (2008) reported that the typical lignin linkages of β - β , β -1, and β -5 types can also be formed by coupling reaction under slightly acidic conditions. The crude lignins separated by RVET and AT, being justified as HSG and S lignin, respectively, were also supported by the aforementioned FTIR spectra.

Table 4. $^1\text{H-NMR}$ Spectra of Lignin Dissolved in DMSO- d_6

δ (ppm)	Assignment	Evaporative Precipitate	Acid Precipitate
9.53~9.78	H of conjugated carbonyl	9.53~9.78	-
8.27~8.29	H of phenolic hydroxyl groups	8.27~8.29	-
7.49~7.76	Aromatic proton in p-hydroxy phenyl units	7.49~7.76	-
7.20	Aromatic proton in guaiacyl units	7.20	-
6.59~6.79	Aromatic proton in syringyl units	6.59~6.78	6.77~6.79
4.49	H_α & H_β of β -O-4 structures, and H_α of β - β structures	4.49	-
4.24~4.26	H_γ of β -1, β -5, β -O-4, and β - β structures	-	4.24~4.26
3.34~3.74	H of methoxyl groups	3.34~3.74	3.35~3.74
1.60~2.22	H of aliphatic acetates	1.60~2.22	1.60~2.22

TGA

The TGA and derivative TGA (DTGA) curves of acid and evaporative precipitate at a heating rate of 15 $^\circ\text{C}/\text{min}$ under N_2 are shown in Fig 3. The mass loss at low temperature (around 100 $^\circ\text{C}$) was due to water vaporization. The maximum thermal decomposition temperatures and the final carbon residues of evaporative and acid precipitate were 520 $^\circ\text{C}$, 5.26%, and 470 $^\circ\text{C}$, 27.92%, respectively. Compared with evaporative precipitate, acid precipitate had a higher final carbon residue (27.92%), lower maximum degradation temperature (470 $^\circ\text{C}$), and narrower maximum peak of the DTGA curve, which indicated the crude lignin separated by AT was more likely to have higher lignin content, smaller molecular weight, and homogeneous lignin. Liu (2009) reported that the maximum thermal degradation of lignin and cellulose under a narrow temperature range 350 $^\circ\text{C}$ to 450 $^\circ\text{C}$ and 280 $^\circ\text{C}$ to 290 $^\circ\text{C}$, respectively, and hemicelluloses were mostly degraded at the initial thermal degradation stage of cellulose. As shown in Fig 3, slight shoulder peaks of DTGA ascribed to pyrolysis of the degradation of carbohydrate in evaporative and acid precipitate were found around 258 $^\circ\text{C}$ and 294 $^\circ\text{C}$, respectively. The differences confirmed that the structures of crude lignin of the PHL were substantially affected by preparation method. The previous studies have been well documented that the lignin removal/precipitation via acidification was significantly affected by the structure/functional groups and molecular weight of the dissolved lignin in the PHL (Yang *et al.* 2013).

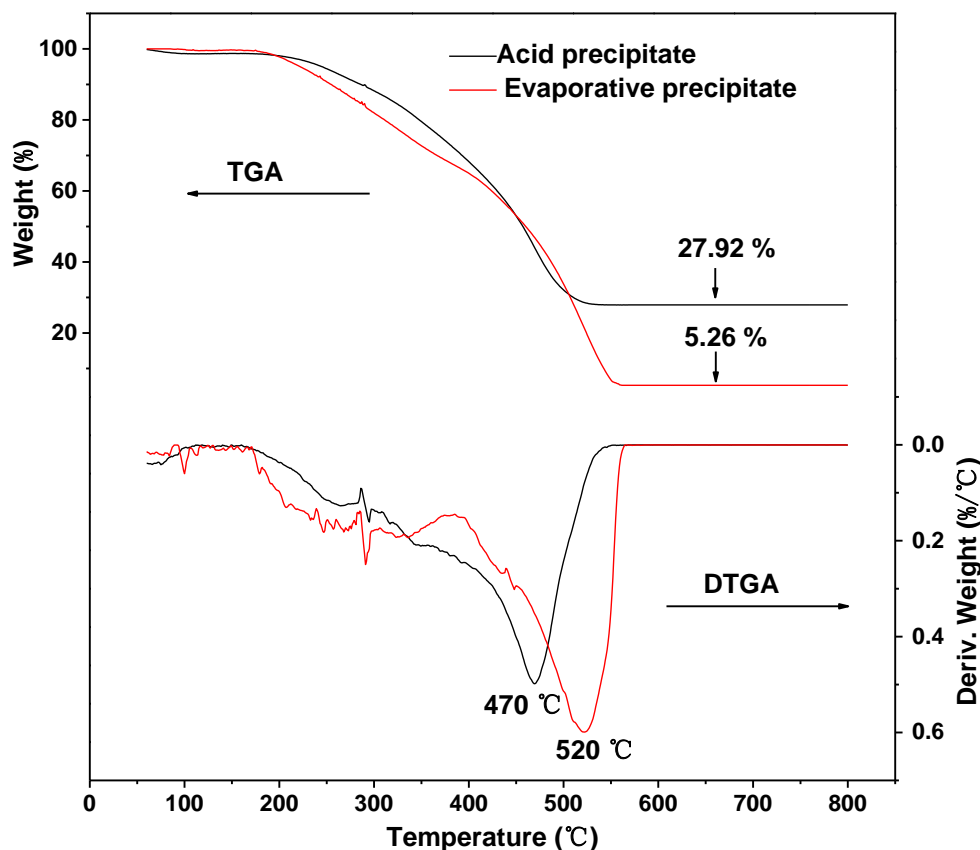


Fig. 3. TGA/ DTGA curves of acid and evaporative precipitate, as crude lignin separated by AT and RVET from PHL, respectively

Py-GC/MS

Based on the TGA results, the temperatures in the pyrolysis of acid and evaporative precipitate were programmed at 650 °C and 800 °C, respectively. The pyrolysis products are shown in Table 5. Pyrolysis is the direct thermal decomposition of the organic materials in the absence of oxygen to obtain an array of gas, liquid, and solid products (Liu *et al.* 2016). Many studies have indicated that pyrolysis is a promising thermo-chemical route to convert lignin into different valuable products (Hu *et al.* 2013). Furthermore, Ibarra *et al.* (2004) reported that Py-GC/MS is a powerful analytical tool for the rapid analysis of lignocellulosic materials. As shown in Table 5, pyrolysis products of acid and evaporative precipitate contained large quantities of methoxy group at 650 °C, which may be related to the large amounts of syringyl lignin in the PHL as indicated by FTIR and $^1\text{H-NMR}$ analysis. In addition, micromolecule compounds, *e.g.*, phenol and ethylbenzene were increased in pyrolysate at temperature up to 800 °C. Especially, the benzene was identified in pyrolysate at temperature up to 800 °C. However, the contents of macromolecule compounds, *e.g.*, d-limonene and 2-methoxy-phenol were decreased at 800 °C. This may be explained as the macromolecule compounds were further broken into fragments besides multi-degradation at high temperature (Huang *et al.* 2012). The results in Table 5 also show that the phenolic aldehyde group, methoxyl, and side chain hydroxyl of the syringyl and guaiacyl lignin were reduced, and a large amount of substituted methyl, ethenyl, and ethyl phenol were produced at pyrolysis temperature 800 °C.

Table 5. Identified Pyrolysis Products of Acid and Evaporative Precipitate, as Crude Lignin Separated by AT and RVET from PHL Respectively, at Various Temperatures

Reaction Time (min)	Compound	Relative Peak Area (%)			
		Acid Precipitate		Evaporative Precipitate	
		650	800	650	800
2.243	Benzene	-	7.12	-	9.73
3.089	Spiro[2,4]hepta-4,6-diene	-	7.89	4.78	12.63
3.095	Hydrazinecarboxylic acid, phenylmethyl ester	6.52	-	-	-
3.923	1,2-Cyclohexanedimethanol	3.56	0.97	-	-
4.24	Ethylbenzene	-	1.83	-	2.90
4.345	<i>p</i> -Xylene	-	2.66	-	-
4.348	<i>o</i> -Xylene	-	-	0.97	3.22
5.974	Phenol	12.74	14.38	10.98	12.77
6.74	D-limonene	3.33	3.24	3.42	-
7.117	2-Methyl-phenol	3.11	4.06	2.94	4.74
7.43	<i>p</i> -Cresol	12.76	13.94	10.20	13.23
7.693	2-Methoxy-phenol	10.63	-	11.61	-
8.554	2,4-Dimethyl-phenol	-	1.85	-	-
8.563	3,5-Dimethyl-phenol	-	-	-	1.92
8.564	4-(2,5-Dihydro-3-methoxyphenyl) butylamine	-	-	2.30	-
8.825	4-Ethyl-phenol	-	4.02	-	4.50
8.841	2-Ethyl-phenol	4.58	-	3.27	-
9.247	2,5-Dimethyl-1,4-benzenediol	5.80	2.24	-	-
9.251	Creosol	-	-	4.06	-
9.6	2,3-Dihydro-benzofuran	18.67	11.01	16.51	24.98
10.98	2-Methyl-5-(1-methylethyl)-phenol	-	8.66	-	9.37
10.985	2-Methoxy-4-vinylphenol	15.44	-	15.27	-
11.506	2,6-Dimethoxy-phenol	-	-	13.66	-
15.681	2,6-Dimethoxy-4-(2-propenyl)-phenol	1.80	4.39	-	-
16.103	1-(4-Hydroxy-3,5-dimethoxyphenyl)-ethanone	1.03	7.56	-	-
18.952	<i>i</i> -Propyl 14-methyl-pentadecanoate	-	1.34	-	-
19.909	Heptadecanoic acid, 16-methyl-, methyl ester	-	2.83	-	-

CONCLUSIONS

1. The crude lignin separated by rotary vacuum evaporation treatment (RVET) could be justified as *p*-hydroxyphenyl-syringyl-guaiacyl (HSG) lignin with conjugated carbonyl functional groups also found in it, while the crude lignin separated by acidification treatment (AT) was mainly composed of S lignin that had β -1, β -5, β -O-4, and β - β bonds.
2. Thermogravimetric analysis (TGA) results showed that the maximum thermal decomposition temperatures and the final carbon residues of crude lignin separated by RVET and AT were 520 °C, 5.26%, and 470 °C, 27.92%, respectively. The differences

confirmed that the structures of crude lignin of prehydrolysis liquor (PHL) were substantially affected by preparation method.

3. Only the contents of galactose and glucose among the five kinds of sugar (arabinose, galactose, glucose, xylose and mannose) in the PHL were decreased after AT, while all five kinds of sugar contents in the PHL were decreased after RVET.

ACKNOWLEDGMENTS

The authors gratefully acknowledge financial support from the Shandong Province Department of Education Fund (No. J14LD01) and the Project of Scientific Development Program in Shandong Province (No. 2014GGX108003).

REFERENCES CITED

- Batalha, L. A. R., Colodette, J. L., Gomide, J. L., Barbosa, L. C. A., Maltha, C. R. A., and Gomes, F. J. B. (2011). "Dissolving pulp production from bamboo," *BioResources* 7(1), 640-651. DOI: 10.15376/biores.7.1.0640-0651
- Buta, J. G., Zadrazil, F., and Galleti, G. C. (1989). "FT-IR determination of lignin degradation in wheat straw by white rot fungus *Stropharia rugosoannulata* with different oxygen concentrations," *Journal of Agricultural and Food Chemistry* 37(5), 1382-1384. DOI: 10.1021/jf00089a038
- Chen, X., Wang, Z., Fu, Y., Li, Z., and Qin, M. (2014). "Specific lignin precipitation for oligosaccharides recovery from hot water wood extract," *Bioresource Technology* 152(1), 31-37. DOI: 10.1016/j.biortech.2013.10.113
- Christov, L. P., and Prior, B. A. (1993). "Xylan removal from dissolving pulp using enzymes of *Aureobasidium pullulans*," *Biotechnology Letters* 15(12), 1269-1274. DOI: 10.1007/bf00130310
- Constant, S., Basset, C., Dumas, C., Di Renzo, F., Robitzer, M., Barakat, A., and Quignard, F. (2015). "Reactive organosolv lignin extraction from wheat straw: Influence of Lewis acid catalysts on structural and chemical properties of lignins," *Industrial Crops and Products* 65, 180-189. DOI: 10.1016/j.indcrop.2014.12.009
- Hu, J., Xiao, R., Shen, D., and Zhang, H. (2013). "Structural analysis of lignin residue from black liquor and its thermal performance in thermogravimetric-Fourier transform infrared spectroscopy," *Bioresource Technology* 128, 633-9. DOI:10.1016/j.biortech.2012.10.148
- Huang, Y., Wei, Z., Qiu, Z., Yin, X., and Wu, C. (2012). "Study on structure and pyrolysis behavior of lignin derived from corncob acid hydrolysis residue," *Journal of Analytical and Applied Pyrolysis* 93, 153-159. DOI: 10.1016/j.jaap.2011.10.011
- Ibarra, D., Río, J. C. d., Gutiérrez, A., Rodríguez, I. M., Romero, J., Martínez, M. a. J., and Martínez, Á. T. (2004). "Isolation of high-purity residual lignins from eucalypt paper pulps by cellulase and proteinase treatments followed by solvent extraction," *Enzyme and Microbial Technology* 35(2-3), 173-181. DOI: 10.1016/j.enzmtec.2004.04.002
- Jahan, M. S., and Mun, S. P. (2007). "Characteristics of dioxane lignins isolated at different ages of nalita wood (*Trema orientalis*)," *Journal of Wood Chemistry and Technology* 27(2), 83-98. DOI: 10.1080/02773810701486865

- Leschinsky, M., Zuckerstätter, G., Weber, H. K., Patt, R., and Sixta, H. (2008). "Effect of autohydrolysis of eucalyptus globulus wood on lignin structure. Part 1: Comparison of different lignin fractions formed during water prehydrolysis," *Holzforschung* 62(6), 645-652. DOI: 10.1515/hf.2008.117
- Li, H. (2016). *Isolation and Struction Characterization of Lignin and Hemicelluloses from Crop Straw*, Master's Thesis, Agricultural and Forest Biomass Utilization. Shanxi, China.
- Liu, G., and Duan, X. (1996). "Appilication of ^1H , ^{13}C nuclear magnetic resonance spectroscopy on the lignin chemistry," *Journal of Jilin Forestry University* 12(4), 239-243.
- Liu, Q. (2009). *Biomass Pyrolysis Mechanism Based on the Multi-components*, Ph.D. Dissertation, Zhejiang University, Zhejiang, China.
- Liu, Y., Liu, Y., Lyu, G., Ji, X., Yang, G., Chen, J., and Lucia, L. A. (2016). "Analytical pyrolysis pathways of guaiacyl glycerol- β -guaiacyl Ether by Py-GC/MS," *BioResources* 11(3), 5816-5828. DOI: 10.15376/biores.11.3.5816-5828
- Lundquist, K., Mannervik, B., Nordfors, K., Nishida, T., and Enzell, C. (1979). "NMR studies of lignins. 3. ^1H NMR spectroscopic data for lignin model compounds," *Acta Chemica Scandinavica* 33b, 418-420. DOI: 10.3891/acta.chem.scand.33b-0418
- Nigam, J. N. (2001). "Ethanol production from hardwood spent sulfite liquor using an adapted strain of *Pichia stipitis*," *Journal of Industrial Microbiology & Biotechnology* 26(3), 145-150. DOI: 10.1038/sj.jim.7000098
- Shen, J., Fatehi, P., Soleimani, P., and Ni, Y. (2011). "Recovery of lignocelluloses from pre-hydrolysis liquor in the lime kiln of kraft-based dissolving pulp production process by adsorption to lime mud," *Bioresource Technology* 102(21), 10035-10039. DOI: 10.1016/j.biortech.2011.08.058
- Shi, H., Fatehi, P., Xiao, H., and Ni, Y. (2011). "A combined acidification/PEO flocculation process to improve the lignin removal from the pre-hydrolysis liquor of kraft-based dissolving pulp production process," *Bioresource Technology* 102(8), 5177-82. DOI: 10.1016/j.biortech.2011.01.073
- Shi, Z. J., Xiao, L. P., Deng, J., and Sun, R. C. (2013). "Isolation and structural characterization of lignin polymer from *Dendrocalamus sinicus*," *BioEnergy Research* 6(4), 1212-1222. DOI:10.1007/s12155-013-9321-8
- Shuai, L., Amiri, M. T., Questell-Santiago, Y. M., Héroguel, F., Li, Y., Kim, H., Meilan, R., Chapple, C., Ralph, J., and Luterbacher, J. S. (2016). "Formaldehyde stabilization facilitates lignin monomer production during biomass depolymerization," *Science* 354(6310), 329-333. DOI: 10.5061/dryad.jm8s7
- TAPPI UM 250 (2000). "Acid-soluble lignin in wood and pulp," TAPPI Press, Atlanta, GA.
- Tong, R., Wu, C., Zhao, C., and Yu, D. (2016). "Effect of boric acid addition on the prehydrolysis of whangee," *BioResources* 11(4), 9628-9637. DOI: 10.15376/biores.11.4.9628-9637
- Wang, Q., Jahan, M. S., Liu, S., Miao, Q., and Ni, Y. (2014). "Lignin removal enhancement from prehydrolysis liquor of kraft-based dissolving pulp production by laccase-induced polymerization," *Bioresource Technology* 164, 380-385. DOI: 10.1016/j.biortech.2014.05.005
- Wang, X., Zhuang, J., Jiang, J., Fu, Y., Qin, M., and Wang, Z. (2015a). "Separation and purification of hemicellulose-derived saccharides from wood hydrolysate by

- combined process,” *Bioresour Technol* 196, 426-30. DOI: 10.1016/j.biortech.2015.07.064
- Wang, Z., Wang, X., Fu, Y., Yuan, Z., and Qin, M. (2015b). “Saccharide separation from wood prehydrolysis liquor: Comparison of selectivity toward non-saccharide compounds with separate techniques,” *RSC Advances* 5(37), 28925-28931. DOI: 10.1039/c4ra17017b
- Wen, J. L., Sun, S. L., Xue, B. L., and Sun, R. C. (2015). “Structural elucidation of inhomogeneous lignins from bamboo,” *International Journal of Biological Macromolecules* 77, 250-9. DOI:10.1016/j.ijbiomac.2015.03.044
- Yang, G., and Jahan, M. (2013). “Structural characterization of pre-hydrolysis liquor lignin and its comparison with other technical lignins” *Current Organic Chemistry* 17, 1589-1595. DOI: 10.2174/13852728113179990068
- Yuan, Z., Kapu, N. S., Beatson, R., Chang, X. F., and Martinez, D. M. (2016). “Effect of alkaline pre-extraction of hemicelluloses and silica on kraft pulping of bamboo (*Neosinocalamus affinis* Keng),” *Industrial Crops and Products* 91, 66-75. DOI: 10.1016/j.indcrop.2016.06.019
- Yuan, Z., Wen, Y., Kapu, N. S., Beatson, R., and Mark Martinez, D. (2017). “A biorefinery scheme to fractionate bamboo into high-grade dissolving pulp and ethanol,” *Biotechnology for Biofuels* 10(1). DOI: 10.1186/s13068-017-0723-2
- Zhang, B. (2016). *Structural Characterization of Hemicelluloses and LCC Preparations Extracted from Neosinocalamus affinis*, Master's Thesis, Beijing Forestry University, Beijing, China.
- Zhao, J., Xiuwen, W., Hu, J., Liu, Q., Shen, D., and Xiao, R. (2014). “Thermal degradation of softwood lignin and hardwood lignin by TG-FTIR and Py-GC/MS,” *Polymer Degradation and Stability* 108, 133-138. DOI: 10.1016/j.polymdegradstab.2014.06.006
- Zhao, L., Yuan, Z., Kapu, N. S., Chang, X. F., Beatson, R., Trajano, H. L., and Martinez, D. M. (2017). “Increasing efficiency of enzymatic hemicellulose removal from bamboo for production of high-grade dissolving pulp,” *Bioresour Technol* 223, 40-46. DOI: 10.1016/j.biortech.2016.10.034
- Zheng, M., Li, L., Zheng, M., Wang, X., Ma, H., and Wang, K. (2012). “Effect of alkali pretreatment on cellulosic structural changes of corn stover,” *Environmental Science & Technology* 35(6), 27-31. DOI: 10.3969/j.issn.1003-6504.2012.06.007
- Zhou, Z., Cheng, Y., Zhang, W., Jiang, J., and Lei, F. (2016). “Characterization of lignins from sugarcane bagasse pretreated with green liquor combined with ethanol and hydrogen peroxide,” *BioResources* 11(2), 3191-3203. DOI: 10.15376/biores.11.2.3191-3203

Article submitted: July 4, 2017; Peer review completed: September 4, 2017; Revised version received and accepted: September 14, 2017; Published: September 19, 2017. DOI: 10.15376/biores.12.4.8217-8229